Molecular Catalysis 553 (2024) 113713

Contents lists available at ScienceDirect

Molecular Catalysis

journal homepage: www.journals.elsevier.com/molecular-catalysis

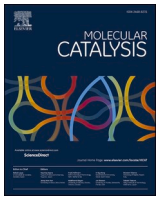

A novel and thermostable phenylalanine dehydrogenase for efficient synthesis of bulky aromatic amino acids and derivatives

Yudong Hu, Guochao Xu, Ye Ni *

Key Laboratory of Industrial Biotechnology, Ministry of Education, School of Biotechnology, Jiangnan University, Wuxi 214122, Jiangsu, China

ARTICLE INFO

Keywords:
Phenylalanine dehydrogenases
Genome mining
Thermostability
Chiral intermediates
2-chloro-L-phenylalanine

ABSTRACT

Phenylalanine dehydrogenases (PDHs) play an important role in pharmaceutical and fine chemical industries due to their ability to produce primary amines via asymmetrically reductive amination. However, the industrial application of PDHs are often limited by their undesirable stability, narrow substrate specificity, especially for unnatural substrates. Here, a novel PDH from *Quasibacillus thermotolerans* (*Qt*PDH) was identified by gene mining using *Bb*PDH from *Bacillus badius* as a probe. *Qt*PDH exhibits prominent thermal stability, specifically a half-life of 23 days at 30 °C and pH 8.5, about 300 times longer than that of *Bb*PDH. *Qt*PDH could catalyze various phenylpyruvate analogues, including ethyl 2-oxo-4-phenylbutyrate and l-phenylglycinol, as well as bulky 3-(naphthalen-1-yl)-2-oxopropanoic acid with a reductive amination specific activity of 1.90 $U \cdot mg^{-1}$. Catalyzed by *Qt*PDH in couple with *Bm*GDH, efficient production of 2-chloro-L-phenylalanine was achieved at 1.0 M 3-(2-chlorophenyl)-2-oxopropionic acid with > 99 % conversion, 99 % *ee*, and space-time yield of 30.46 $g \cdot L^{-1} \cdot h^{-1}$. Our results suggest that this newly identified *Qt*PDH features high catalytic efficiency and thermostability, and is a promising biocatalyst for the industrial productions of bulky aromatic primary amines.

1. Introduction

Aromatic chiral amino acids and their derivatives possess a wide range of structural and functional diversity, and have multiple applications in pharmaceutical, agrochemical, and food industries [1,2]. As shown in Scheme 1, (*S*)-indolein-2-carboxylic acid (**3**) is a key chiral building block for the synthesis of angiotensin-converting enzyme inhibitors (ACEI) Perindopril and Indolapril. And the use of inexpensive copper catalysis for intramolecular cyclization of ortho-halophenylalanines has become a primary method for the synthesis of (**3**), with exceeding 99 % *ee*. Among all ortho-halophenylalanines, 2-Cl-Phe is a desirable choice in terms of cost and waste disposal [3–5]. In addition, 2-Cl-Phe is also commonly used for the synthesis of functional oligopeptides [6]. With the growing demand for aromatic amino acid derivatives, there is an urgent need for the development of efficient production approaches [7]. As an alternative to chemical synthesis, biocatalysis has emerged as a sustainable and efficient approach for the synthesis of aromatic amino acid derivatives [8].

Among biocatalytic methods used for this purpose, transaminases, phenylalanine ammonia lyases (PALs), and phenylalanine dehydrogenases (PDHs) are the most commonly employed enzymes. Transaminases are versatile enzymes utilizing pyridoxal 5′-phosphate (PLP) as co-factor to transfer amino groups from amine donors to acceptors. However, transaminases catalyzed reactions often require excessive amine donors, leading to complicated product extraction. Besides, the by-product generated after deamination of amine donor is not favorable in perspective of atomic economy [9–11]. PALs catalyze the deamination of L-phenylalanine to cinnamic acid, and their reverse addition reaction can be used to synthesize l-phenylalanine derivatives. PAL from *Rhodotorula glutinis* has been reported to produce 2-Cl-Phe with a space-time yield (STY) of 234.59 $g \cdot L^{-1} \cdot d^{-1}$ using substrate feeding strategy [3,12,13]. However, excessive ammonia is required to drive the reverse addition reaction, and achieving strict stereoselectivity for various products is also challenging [14,15].

PDHs utilize NADH/NAD(P)H as cofactor to catalyze the asymmetric reductive amination of aromatic keto acids. Compared with transaminases and PALs, PDHs exhibit high reductive amination activity while maintain strict *S*-selectivity in product configuration. In previous works, PDHs from different sources have been applied in combination with glucose dehydrogenase (GDH) for producing L-homophenylalanine [16,17], *p*-fluorophenylalanine [18] and other derivatives [19], while

* Corresponding author.
E-mail address: yni@jiangnan.edu.cn (Y. Ni).

https://doi.org/10.1016/j.mcat.2023.113713
Received 29 July 2023; Received in revised form 24 October 2023; Accepted 15 November 2023
Available online 23 November 2023

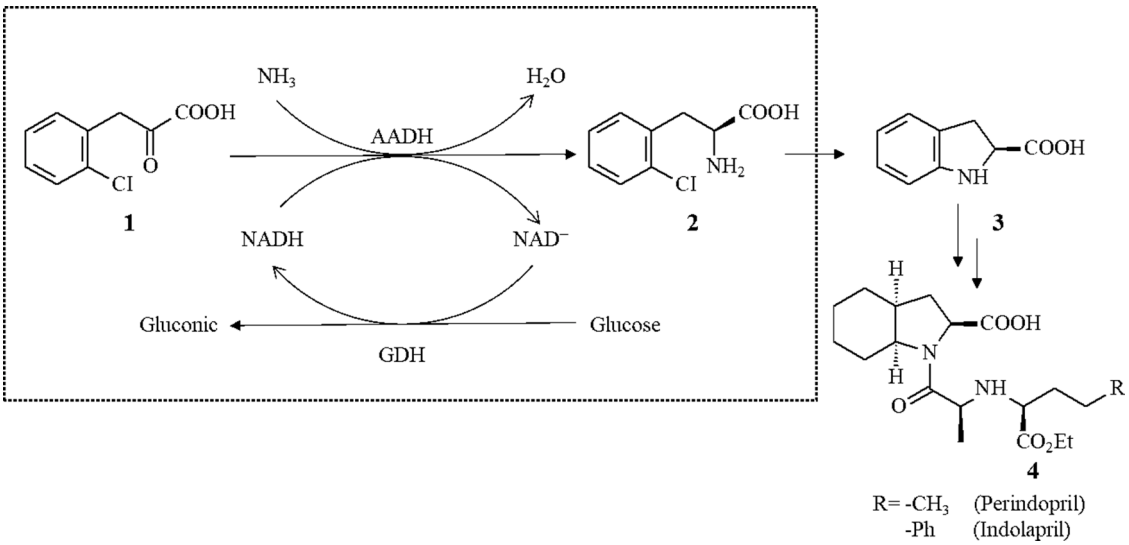

Scheme 1. Asymmetric amination of 3-(2-chlorophenyl)-2-oxopropionic acid (**1,** CPOA) to produce 2-chloro-l-phenylalanine (**2,** 2-Cl-Phe) catalyzed by amino acid dehydrogenase, and several ACE inhibitors with **3** as intermediate.

the production of 2-Cl-Phe has not been reported. PDHs generally have low activity toward unnatural substrates [20], and have poor stability under alkaline pHs. For instance, *Bb*PDH from *Bacillus badius* lost 25 % of its activity after incubation at 30 °C and pH 8.0 for 1 h [21], which is not conducive to industrial production. Therefore, exploring novel PDHs with broad substrate spectrum and high stability is critical for the production of aromatic chiral amino acids and their derivatives.

Here, we attempted to identify potential PDHs for the efficient synthesis of chiral amino acids derivatives. Based on gene mining, *Qt*PDH from *Quasibacillus thermotolerans* was discovered and characterized with excellent activity and stability. Under optimized conditions, efficient production of 2-Cl-Phe catalyzed by *Qt*PDH was achieved, demonstrating its potential for industrial application.

2. Material and methods

2.1. Chemicals, plasmids and strains

N-acetylglycine, hydantoin, ethanolamine, and 2-chlorobenzaldehyde for the synthesis of 3-(2-chlorophenyl)-2-oxopropanoic acid were purchased from Shanghai Merck Biochemical Co., Ltd (Shanghai, China). NADH and NAD^+ were purchased from Bontac Bioengineering company (Shenzhen, China). Other chemicals and reagents were purchased from various commercial sources.

Escherichia coli BL21(DE3) and pET-28a preserved in our laboratory were used for recombinant expression of the enzymes. Genes encoding for the mined enzymes were synthesized by Tianlin Biotechnology Co., Ltd (Wuxi, China). Glucose dehydrogenase (GDH) gene from *Bacillus megaterium* was cloned into pET-28a for expression in *E. coli* BL 21(DE3) [22].

2.2. Recombinant expression of amino acid dehydrogenase genes

Recombinant plasmid pET-28a-*Qt*PDH was constructed and transformed into competent *E. coli* BL21(DE3), followed by spread on LB plate supplemented with 50 $\mu g \cdot mL^{-1}$ kanamycin and incubated at 37 °C for 12 h. Positive colony identified by colony PCR and sequencing was transferred to LB liquid medium supplemented with 50 $\mu g \cdot mL^{-1}$ kanamycin and cultivated at 37 °C and 180 rpm overnight. Then, 1 mL culture was inoculated into 100 mL fresh LB medium containing 50 $\mu g \cdot mL^{-1}$ kanamycin for further growth. When the optical density (OD_{600}) reached 0.6–0.8, 0.2 mM IPTG (final concentration) was added to induce expression at 16 °C and 180 rpm for further 18 h. After centrifugation (4 °C, 8000 rpm, 10 min), the collected cells were freeze-dried, and the dry cell powder was stored at 4 °C for further use.

2.3. General method for activity assay

For most substrates, the activity of amination and deamination was measured by monitoring the absorbance change at 340 nm (corresponding to the coenzyme NADH ($\varepsilon = 6220\ M^{-1}cm^{-1}$)) during the initial reaction. The typical 200 μL reaction system for activity measurement consisted of buffer, 2 mM substrate, 1 mM NADH/NAD^+, a certain amount of target enzyme and was measured at 30 °C. NH_4Cl/NH_4OH buffer (1 M, pH 9.0) and Glycine/NaOH buffer (0.5 M, pH 10.5) were used for amination and deamination reactions respectively. One unit of enzyme activity (1 U) was defined as the amount of enzyme required to consume (for amination) or produce (for deamination) 1 μmol NADH per minute. For several substrates exhibiting strong absorption at 340 nm, HPLC was used to determine the activity. The enzyme concentration was calculated by Bradford Assay.

2.4. Determination of enantioselectivity in amination reactions

A 1 mL reaction system containing *Qt*PDH enzymes (lyophilized cell-free extract 1.5 mg), NAD^+ (1 mM), substrate (2 mM), ethanol (5 % v/v), glucose, GDH (lyophilized cell-free extract 2.5 mg), and buffer (NH_4Cl/NH_4OH, 1 M, pH 9.0) was incubated at 30 °C and 180 rpm for 2 h. The reaction was then quenched by boiling water bath for 10 min. After centrifugation (12,000 rpm, 5 min), the supernatant was collected. Samples were diluted and filtered (0.22 μm), and then analyzed by HPLC equipped with Astec CHIROBIOTIC™ T column (150 × 4.6 mm, 5 μm). The analytical condition for 2-Cl-Phe was methanol: H_2O (70:30), column temperature 35 °C, flow rate 0.8 $mL \cdot min^{-1}$, and detection wavelength of 222 nm. The retention times of (*R*)- and (*S*)- 2-Cl-Phe were 4.42 min and 4.00 min, respectively (**Figure S1**).

2.5. Enzyme purification

Freeze-dried cells were resuspended in affinity buffer (20 mM imidazole, 500 mM NaCl, 20 mM Tris-HCl buffer and pH 8.0), and disrupted using an ultrasonic crusher (350 W, working 2 s and resting 3 s for 10 min) in an ice-water bath. The cell lysate was centrifuged at 8000 rpm for 30 min, and the resulting supernatant was filtered through a

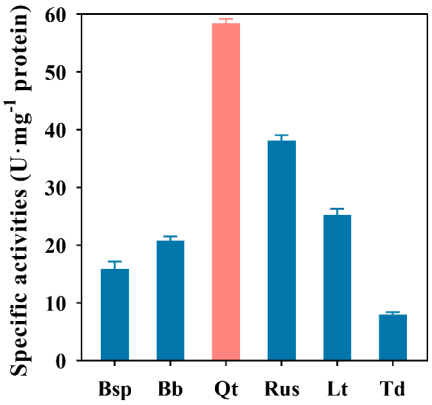

Fig. 1. Specific activities of various AADHs toward CPOA. The activity assay was performed by measuring OD_{340} in 2 M $NH_4Cl/NH_3{\cdot}H_2O$ buffer (pH 9.0) containing 1 mM CPOA, 1 mM NADH and appropriate amount of purified enzymes.

0.22 μm filter. Subsequently, the sample was loaded onto a Ni-NTA affinity column (Sangon Biotech Co., Ltd.). The eluates were then collected simultaneously using varying concentrations of imidazole buffer ranging from 20 to 500 mM. The elution fractions containing the target protein was confirmed by SDS-PAGE analysis (**Figure S2**), and were concentrated by ultrafiltration. Finally, the affinity buffer was replaced by Tris-HCl buffer (100 mM, pH 8.5) using desalting column. The protein concentration of the pure enzyme was measured using Nanodrop 2000c (Thermo Electron Co., Ltd.), and the data utilized in the measurements were provided by ExPASy ProtParam Tool [23]. The purified enzyme was stored at −80 °C for further use.

2.6. Enzyme characterization of purified QtPDH

2.6.1. Effect of pH and temperature

Enzymatic activity was measured in buffers with different pHs according to the method 2.3, using 3-(2-chlorophenyl)-2-oxopropionic acid (CPOA)/2-Cl-Phe as the substrate. The buffers with different pHs included NH_4Cl/NH_4OH buffer (pH 8.0–10.0, 1 M), Glycine/NaOH buffer (pH 9.5–11.5, 0.1 M).

To determine the effect of temperature on the enzyme activity, the enzyme activity was determined at 25 to 60 °C. Following the general activity assay 2.3, the reaction system was first kept at different temperatures (25, 30, 40, 50, 60 °C) for 20 min, and then the enzyme was added to start the reaction, while the absorbance change of OD_{340} was recorded.

The highest activity measured for each enzyme was defined as 100 %, and then the relative activity of the enzyme at different pHs/temperatures was calculated sequentially. At least three replicate experiments were performed for each data set.

2.6.2. Metal ion dependence

Effect of different metal ions on the enzyme activity was evaluated with EDTA, Al^{3+}, Fe^{3+}, Mn^{2+}, Ba^{2+}, Mg^{2+}, Ca^{2+}, Co^{2+}, Ni^{2+}, Fe^{2+}, Cu^{2+}, Zn^{2+}, Ag^{1+} metal ions. Purified *Qt*PDH was diluted appropriately, and EDTA or the metal ions were added to a final concentration of 1 mM. After incubation for 2 h at 30 °C, the residual activity was measured. The reaction without metal ions served as the control group, with its specific activity considered 100 %.

2.6.3. Salt tolerance

The activity of *Qt*PDH was determined according to the method 2.3, except that NaCl was added into NH_4Cl/NH_4OH buffer to final salt concentrations of 0.1, 0.5, 1.5, 2.0, 2.5 M. The reaction system containing 0.1 M NaCl were defined as 100 %.

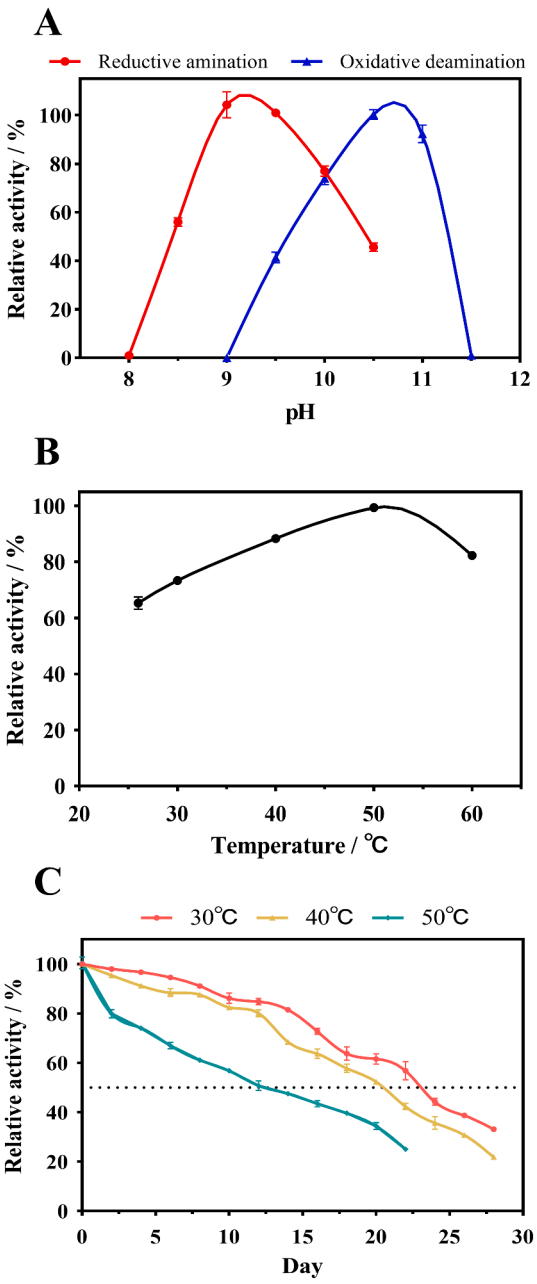

Fig. 2. Effect of pH and temperature on activity and thermostability of *Qt*PDH. A: pH profile, B: temperature profile, C: thermostability.

2.6.4. Thermostability

Thermostability experiments were conducted in two sets. The first set was examined at pH 8.5 (Tris-HCl, 100 mM) and pH 9.5 (Tris-HCl, 100 mM), respectively, under constant temperature of 30 °C; while the second set was investigated at 30 °C, 40 °C and 50 °C. During the experiments, the purified *Qt*PDH was diluted to 1 $mg{\cdot}mL^{-1}$, and then incubated in water bath at 30, 40 and 50 °C in 100 mM pH 8.5 Tris-HCl buffer. During the incubation, samples were taken and bathed in ice for 5 min and then diluted to the appropriate concentration for activity determination. The first sampling time was 5 min after the start of incubation. The relative activity of the subsequent samples was calculated from the first set of data which was considered as 100 %.

2.6.5. Substrate specificity

Specific activity of *Qt*PDH for amination or deamination of different substrates was determined by monitoring OD_{340} as described in method

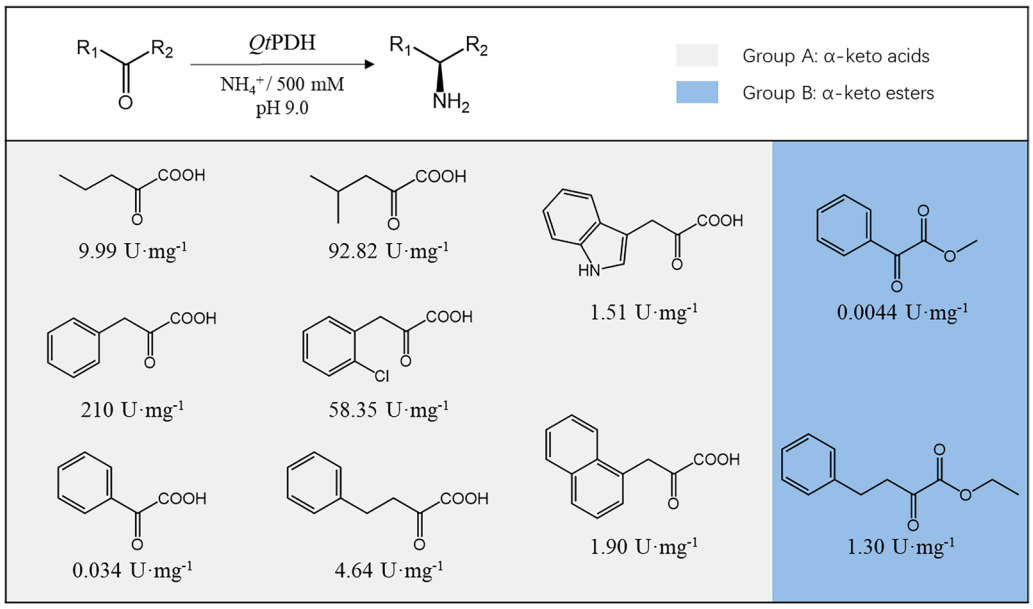

Fig. 3. Substrate specificity in reductive amination of purified *Qt*PDH toward α-keto acids/esters.

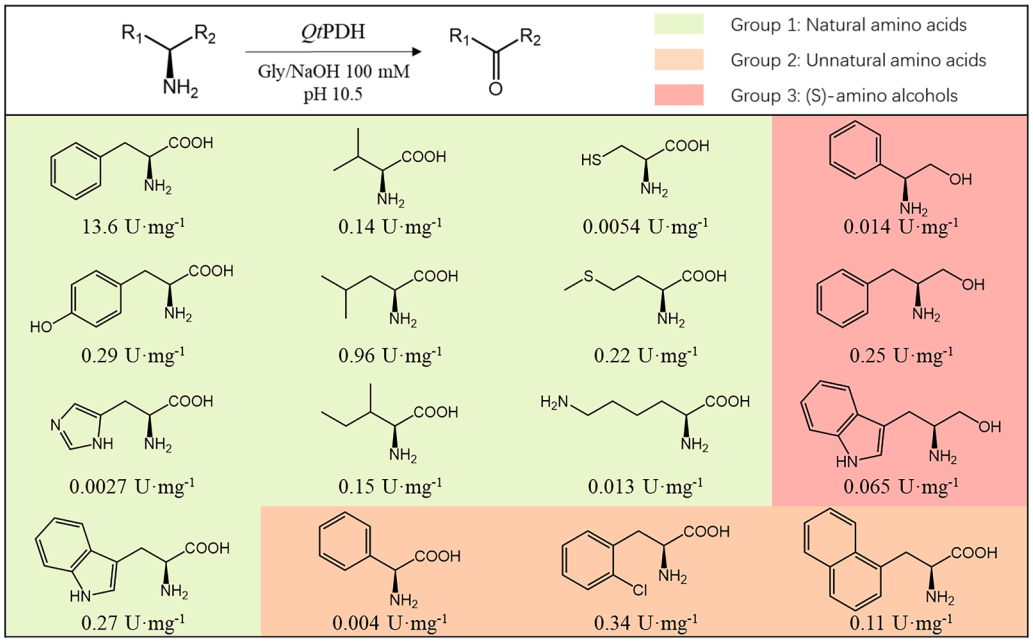

Fig. 4. Substrate specificity in oxidative deamination of purified *Qt*PDH toward various amino acids and amino alcohols.

2.3. For substrates 3-(naphthalen-1-yl)-2-oxopropanoic acid and indole-3-pyruvic acid, HPLC analysis was used. One mL reaction containing 1 mM NADH, 1 mM substrate, and NH_4Cl/NH_4OH buffer (1 M, pH 9.0) was conducted for 10 to 30 min at 30 °C, and analyzed by HPLC. Based on standard curve of the product (**Figure S3**), specific activity was calculated. ZORBAX SB-18 column (15 cm × 4.6 mm × 5.0 μm) was used at following parameters: mobile phase KH_2PO_4 solution (20 mM, pH 2.25) with acetonitrile (20 %), flow rate 0.9 mL·min^{-1} for 25 min at 35 °C, UV detection at 210 nm.

2.6.6. *Kinetic parameters*

Kinetic parameters of purified *Qt*PDH were calculated according to the double-substrate enzyme reaction model. The activity assay was performed as described above. To determine the kinetic parameters of NADH, the reaction was carried out in NH_4Cl/NH_4OH buffer (1 M, pH 9.0) containing 1 mM 2-oxo-keto acid and varying concentration of NADH at 30 °C. In the same way, the kinetic parameters of substrates were measured with varied concentration of 2-oxo-keto acid. The kinetic parameters (K_M and k_{cat}) were obtained by non-linear fitting of initial velocity versus substrate concentration data to the Michaelis-Menten equation using Graphpad prism 8.0.

2.7. *Chemical synthesis of CPOA*

Hydantoin (15 g) was added to a 500 mL three-neck flask containing distilled water (75 mL), and heated to 60 °C to dissolve hydantoin completely. Ethanolamine (7.32 g) was added dropwise within 5 min. Then, the mixture was heated to 90 °C, 2-chlorobenzaldehyde (21 g) was added at a rate of 2.5 mL·min^{-1}, the reaction was carried out at 100 °C for 7 h. The progress of the reaction was monitored by TLC (hexane:

Table 1
Kinetic parameters of amination reactions catalyzed by purified *Qt*PDH toward various substrates.

[S]	K_M (mM)	k_{cat} (s^{-1})	k_{cat}/K_M ($s^{-1}mM^{-1}$)	K_i (mM)
NADH	0.088 ± 0.02	146.30 ± 9.40	1662.50	*n. d.*
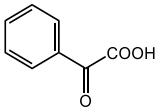	5.16 ± 1.20	0.048 ± 0.0071	0.0093	*n. d.*
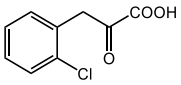	0.51 ± 0.30	58.91 ± 2.11	115.51	0.26
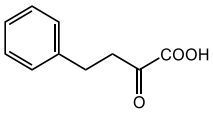	0.19 ± 0.080	0.53 ± 0.046	2.84	*n. d.*

n. d.: no inhibition was determined.

ethyl acetate 1:1 and 1:9). After cooled to room temperature, the reaction was filtered and dried to obtain intermediate products. The intermediate was re-dissolved with sodium hydroxide solution (2.5 M), and the substrate concentration was maintained at 0.5 M for hydrolysis. The reaction was stopped after 3.5 h at 80 °C. After cooling, the pH of the reaction was adjusted to about 5.4 with concentrated HCl solution. After standing crystallization, the product was obtained after filtration [24, 25].

^{1}H NMR (600 MHz, Methanol-d4) δ 8.23 (dd, J = 8.0, 1.8 Hz, 1H), 7.28 (d, J = 8.1 Hz, 1H), 7.16 (t, J = 7.6 Hz, 1H), 7.07 (td, J = 7.6, 1.7 Hz, 1H), 6.80 (s, 1H).

2.8. Asymmetric synthesis of 2-Cl-Phe catalyzed by QtPDH

One mL reaction system contained *Qt*PDH (lyophilized cell lysate, 1.5 mg), GDH (lyophilized cell lysate, 4 mg), 2 mM substrate, NAD^+ (1 mM), and NH_4Cl/NH_4OH buffer (1 M, pH 8.5). The reaction was conducted at 30 °C and 180 rpm for 1−12 h. Optimization of the reaction system with a total volume of 65 mL was performed based on *Qt*PDH loading of 1 kU which corresponds to 65 mg lyophilized cell lysate (65 mg × 15 U/mg ≈ 1 kU). The reaction system consisted of 10 mL of reaction mixture, 50 mL of CPOA feeding solution, and 5 mL ammonia. The 10 mL reaction mixture contained *Qt*PDH (lyophilized cell lysate, 65 mg), GDH (lyophilized cell lysate, 200 mg), NAD^+ (1 mM), and NH_4Cl/NH_4OH buffer (1 M, pH 8.5). The substrate feeding solution was prepared by dissolving CPOA in NH_4Cl/NH_4OH buffer and adjusting the pH to 8.5 with a concentration range from 0.25−1.5 M. The total moles of glucose is 1.2 times that of substrate, where 20 % glucose is dissolved in a 10 mL reaction mixture and 80 % is dissolved in substrate feeding solution. The reaction was conducted in a 250-mL three-neck flask with mechanical stirring at 30 °C and the substrate solution was added with a dripping funnel. The pH of the reaction system was maintained at 8.5 with ammonia.

During the reaction, 500 μL reaction solution was sampled every 20 min, and the samples were subjected to HPLC analysis as described in method 2.6.5 for determining the residual substrate. The conversion ratio was calculated using the following formula.

$$\text{Conv}\ (\%) = 1 - \frac{(V_1 + V_2 + V_3) \times c_1}{V_3 \times c_2} \times 100\%$$

The volume of the reaction system is comprised of three components during the reaction: V_1 represents the initial volume, V_2 denotes the supplemented ammonia volume determined by visual inspection of titrator scale degree, and V_3 signifies the feeding substrate volume calculated as a product of sampling time and flow rate. c_1 refers to real-time substrate concentration obtained from HPLC results while c_2 indicates feeding substrate concentration.

2.9. Scaled-up reaction and recovery of 2-Cl-Phe

The scale-up preparation of 2-Cl-Phe was carried out based on optimized reaction conditions (Entry 3, Table 2) with 10-time scaled-up in equal proportions. An initial reaction system (100 mL) included *Qt*PDH (lyophilized cell lysate, 0.65 g), GDH (lyophilized cell lysate, 2 g), NAD^+ (1 mM), and NH_4Cl/NH_4OH buffer (1 M, pH 8.5) as well as glucose (22 g). The substrate was prepared by chemical hydrolysis, and the pH was adjusted to 8.0 using concentrated hydrochloric acid. A total volume of 500 mL substrate solution (1 M) containing glucose (86 g) was

Table 2
Asymmetric reductive amination of CPOA catalyzed by *Qt*PDH coupled with GDH.

Entry	Substrate ($mol \cdot L^{-1}$)	Total activity (kU)		S/C [c] ($g \cdot g^{-1}$)	Reaction time (h)	Conv (%)	Product [d] ($g \cdot L^{-1}$)	STY ($g \cdot L^{-1} \cdot h^{-1}$)
		*Qt*PDH [a]	*Bm*GDH [b]					
1	0.25	1	2	9.23	2	>99	38.08	19.04
2	0.5	1	2	18.47	3.5	>99	76.15	21.76
3	1.0	1	2	36.94	5	>99	152.31	30.46
4	1.5	1	2	55.41	12	73.5	171.35	14.27
5	1.0	10	20	36.94	11.5	>99	152.31	13.24

[a] Specific activity was about 15 $U \cdot mg^{-1}$ lyophilized cell lysate of *Qt*PDH.
[b] Specific activity was about 10 $U \cdot mg^{-1}$ lyophilized cell lysate of *Bm*GDH.
[c] S/C: substrate to catalyst ratio.
[d] Different concentrations of ammonia were used to maintain the pH of the reaction system and to give a total volume of about 65 mL for entry1−4, and about 650 mL for 5.

added by feeding. Concentrated ammonia water (≈13 M) was used to maintain pH 8.5 and provide ammonium ions.

Here, Fe^{3+} chromogenic method was used to monitor the reaction process (**Figure S4**). Briefly. 0.125 g ferric chloride was dissolved in 100 mL dimethyl sulfoxide, and 5 mL glacial acetic acid was added to a final volume of 250 mL to prepare the chromogenic reagent. First, 100 μL of the chromogenic agent was added into 100 μL appropriately diluted reaction solution, and followed by standing for 15 min, then absorbance at 640 nm was measured using a microplate reader. At the beginning of the reaction, a peristaltic pump was used for substrate feeding at a flow rate of 2 mL/min. The conversion ratio was monitored using Fe^{3+} chromogenesis method to ensure that the OD_{640} value was below 0.3 (< 0.5 mM CPOA).

At the end of the reaction, the pH of the reaction solution was adjusted to 1.0 with concentrated HCl solution. After standing for 30 min, the filtrate was filtered and collected for subsequent product extraction steps. Product 2-Cl-Phe was purified using a JK006 gel-type cationic resin column. The resin was first soaked in NaOH solution, water and HCl solution for 12 h each, and then filled to prepare the resin affinity chromatographic column (100 mm × 50 mm) (**Figure S13 (A)**). The affinity column was washed with deionized water until the effluent was neutral. The reaction solution was diluted to a product concentration of 10–15 $g{\cdot}L^{-1}$, and then loaded into the resin affinity column at a rate of 1 $Bv{\cdot}h^{-1}$. After loading, the resin column was washed with deionized water until the effluent was neutral, and then eluted with ammonia water (1 M). A 0.3 % ninhydrin chromogen reagent (1.5 g of ninhydrin dissolved in 103 mL of *n*-butanol solution containing 3 mL of acetic acid) was used to assist in determining the start and end points of the collection. The collected solution was concentrated by rotary evaporation to remove ammonia and most of the water, then subjected to freeze-drying treatment. After identification by NMR, the purity of the product was calculated based on standard curve as determined by HPLC.

3. Results and discussion

3.1. Mining of amino acid dehydrogenases for amination of 3-(2′-chlorophenyl)-2-oxopropanoic acid

*Bsp*PDH from *Bacillus sphaericus* and *Bb*PDH from *B. badius* have been reported with high activity toward aromatic substrates [20,21,26]. Particularly, remarkable specific activities of 15.2 $U{\cdot}mg^{-1}$ and 21.8 $U{\cdot}mg^{-1}$ toward 3-(2′-chlorophenyl)−2-oxopropionic acid (CPOA) were determined for *Bsp*PDH and *Bb*PDH, respectively. To explore novel amino acid dehydrogenases (AADHs) with high catalytic activity toward CPOA, *Bb*PDH was used as the probe to mine new enzymes from Uniprot database. Four enzymes sharing 53.3−87.6 % identities in amino acid sequence with *Bb*PDH were selected (**Table S1**), and expressed in *E. coli*. Reductive amination activity of purified proteins was determined at different pH values (**Figure S2**). All four enzymes showed activities toward CPOA. Among them, *Qt*PDH from *Quasibacillus thermotolerans* exhibited the highest activity in the amination of CPOA with specific activity of 58.35 $U{\cdot}mg^{-1}$ (Fig. 1). Further analysis of enantioselectivity demonstrated that *Qt*PDH catalyzed the formation of amino acids in absolute *S*-configuration, consistent with the strict selectivity rule of AADHs. (**Figure S1(B)**). Considering the highest activity and enantioselectivity, *Qt*PDH was selected for subsequent studies.

We conducted a sequence alignment of *Qt*PDH with diverse classes of amino acid dehydrogenases. Our findings revealed that the sequence identity between *Qt*PDH and extensively studied phenylalanine dehydrogenases *Bb*PDH was 83.7 %, while between *Qt*PDH and *Rs*PDH [27] was determined to be 32.9 %. Besides, *Qt*PDH shares 49.5 % and 50.2 % sequence identity with *Bc*LeuDH [22] and *Es*LeuDH [28], respectively. Similar to *Bb*PDH, *Qt*PDH has a biased function towards the Glu/Leu/Phe/Val/Trp dehydrogenase family. Furthermore, despite the large differences in sequence identity between *Qt*PDH and its isoenzyme, it has the strict conserved catalytic sites K78, K90, D124 common to all phenylalanine dehydrogenases [29]. We postulated that *Qt*PDH should also be structurally divided into two domains, domain I and domain II, whose intersection forms a catalytic pocket with a cleft shape [30,31].

3.2. Characterization on enzyme properties of QtPDH

Recombinant *Qt*PDH with N-terminal His-tag was purified. SDS-PAGE analysis revealed that *Qt*PDH displayed a single band at about 44.8 kDa (**Figure S2**). As illustrated in Fig. 2A, the optimum pH values for amination and deamination were 9.2 and 10.8, respectively. No deamination activity was detected at pH below 9.0. The effect of temperature was measured over the range of 25 °C to 60 °C (Fig. 2B). The amination activity increased with the temperature, and the highest activity was reached at 52 °C. The relative activity decreased to about 80 % as the temperature further increased to 60 °C.

The specific activity of *Qt*PDH was not affected by EDTA, indicating it is not a metal-dependent enzyme. Addition of 1 mM Mg^{2+} resulted in 15 % increase in activity, while the enzyme was strongly inhibited by 1 mM Fe^{3+}, Fe^{2+}, Cu^{2+}, Zn^{2+}, and Ag^{1+}. The effect of ammonium concentration on specific activity was also investigated. The results showed that with the increase of ammonium concentration from 0 to 2 M, the relative activity rapidly increased to 75 %. Further increase in ammonium to 4 M resulted in a slight increase in activity. Additionally, *Qt*PDH demonstrated good tolerance to NaCl, and no obvious effect was observed in the presence of 0.1–1.5 M NaCl. Whereas, the activity of *Qt*PDH was sharply decreased at 2 M NaCl. (**Figure S5**)

To evaluate its stability, thermostability of *Qt*PDH was determined at pH 8.5 and pH 9.5 at 30 °C (**Figure S6**). The half-lives of *Qt*PDH were 16 days at pH 9.5, and 20 days at pH 8.5. Remarkably, *Qt*PDH was able to maintain significantly high relative activity at pH 8.5 in the initial 10 days, retaining 85 % activity after 10 days at pH 8.5 while only 52 % activity was remained at pH 9.5. This result indicates that pH 8.5 was more suitable for prolonged production. Furthermore, the half-life of *Qt*PDH was determined at 30 °C, 40 °C, and 50 °C at pH 8.5 (Fig. 2C). *Qt*PDH was more stable at 30 °C and 40 °C compared with that of 50 °C. *Qt*PDH exhibited similar half-lives of 23 days at 30 °C and 20.5 days at 40 °C, whereas retained only 50 % activity after 12 days at 50 °C. Interestingly, despite a high sequence identity of 83.7 % with *Bb*PDH, *Qt*PDH displayed significantly better thermostability [20,21,26]. Based on sequence alignment between *Qt*PDH and *Bb*PDH, 13 of the 35 residues differ in polarity/non-polarity, and 22 residues have varied charge (**Figure S7**). It suggests that changes in the polarity and charge properties of surficial residues may severely affect the thermostability of AADHs.

3.3. Substrate spectrum in reductive amination and oxidative deamination of QtPDH

*Qt*PDH showed strict substrate specificity toward phenylpyruvic acid in the reductive amination (Fig. 3). Among benzene homologues including benzoylformic acid, phenylpyruvic acid, and 2-oxo-4-phenylbutyric acid, *Qt*PDH exhibited a noticeably higher amination activity for phenylpyruvic acid of 210 $U{\cdot}mg^{-1}$, while only 0.034 $U{\cdot}mg^{-1}$ and 4.64 $U{\cdot}mg^{-1}$ for other keto acids. Furthermore, *Qt*PDH displayed a specific activity of 58.35 $U{\cdot}mg^{-1}$ for CPOA. *Qt*PDH also demonstrated the ability to catalyze the amination of bulky substrates such as indole-3-pyruvic acid and 3-(naphthalen-1-yl)-2-oxopropanoic acid, with specific activities of 1.51 $U{\cdot}mg^{-1}$ and 1.90 $U{\cdot}mg^{-1}$ respectively. Moreover, *Qt*PDH was able to aminate α-keto ester substrates, such as methyl benzoylformate and ethyl 2-oxo-4-phenylbutyrate, with specific activity of 0.0044 $U{\cdot}mg^{-1}$ and 1.30 $U{\cdot}mg^{-1}$, although lower than that of its keto-acid form.

As shown in Fig. 4, *Qt*PDH could catalyze the oxidative deamination of 10 out of 20 natural amino acids (Fig. 4, Group 1) with the highest deamination activity of 13.6 $U{\cdot}mg^{-1}$ toward l-phenylalanine under the optimal deamination conditions. Notably, *Qt*PDH demonstrated a preference for amination over deamination, as evidenced by its much higher

activity in amination reactions. For example, *Qt*PDH showed activities of 58.35 U·mg^{-1} and 0.34 U·mg^{-1} for the amination and deamination of CPOA, respectively. In addition to the unnatural amino acids, the deamination activity of (*S*)-amino alcohols was also determined (Fig. 4, Group 3). Interestingly, a 3.5-fold greater deamination activity was detected for l-phenylglycinol than l-phenylglycine, suggesting that strong electrostatic interaction between the carboxyl group and the residues in the active pocket is obstructive for rigid substrates. In contrast, a better catalytic conformation could be achieved for l-phenylglycinol due to its flexibility. Other substrates were also evaluated; however, no deamination activity was detected (**Table S2**).

Kinetic parameters of amination reaction toward unnatural amino acids (Fig. 4, Group 2) were determined (Table 1). Among three substrates, 2-oxo-4-phenylbutyric acid has the lowest K_M value of 0.19 mM. For benzoylformic acid, an extremely low k_{cat} value of 0.048 s^{-1} was determined, along with a high K_M value of 5.16 mM, indicating *Qt*PDH prefers keto acid substrates with more flexible residues. Different from benzoylformic acid and 2-oxo-4-phenylbutyric acid, severe substrate inhibition was observed for phenylpyruvate and CPOA. (**Figure S8**)

3.4. Asymmetric synthesis of 2-Cl-Phe catalyzed by QtPDH

Following commonly used methods [24,25,32], synthesis of substrate CPOA was investigated (**Figure S11**). Intermediate 5-[(2-chlorophenyl) methylene]-2,4-imidazolidinedione synthesized from 2-chlorobenzaldehyde and hydantoin could be hydrolyzed under alkaline conditions [24,25], giving a higher separation yield of 72 %. Additionally, the product could be directly added to the enzymatic reaction system after adjusting the pH to 8.0, without the need for extraction.

In the beginning, a 5 ml volume of the reaction was carried out under optimal amination conditions. As shown in **Figure S12**, 200 mM and 300 mm CPOA achieved conversions >90 % at 45 min and 3 h. However, with increasing substrate concentration, the reaction gradually stalled and severe substrate inhibition occurred. At a CPOA loading of 400 mM, the substrate conversion remained at 50 %; at 500 mM, the conversion was 25 %, a result that also corresponds to the consistent substrate inhibition observed during kinetic parameter determination. Similar substrate inhibition has been reported for *Ti*PheDH from *T. intermedius* [33], where high concentrations of substrate may lead to irreversible inactivation of amino acid dehydrogenase.

As mentioned above, with high enzyme loadings (S/C of 1.3 and 1.9), good conversion ratios (> 90 %) were achieved at 200 mM and 300 mM CPOA, inevitably leading to viscous reaction system and low mass transfer efficiency. Therefore, substrate feeding strategy was adopted to alleviate the inhibitory effect of CPOA. The reaction conditions were optimized based on a total *Qt*PDH loading of 1 kU (i.e. 65 mg lyophilized cell lysate). To optimize the reaction, various influential factors, including substrate feeding rate, *Qt*PDH and *Bm*GDH ratio, substrate to catalyst ratio (S/C) etc., were evaluated. Appropriate substrate feeding rate can ensure a complete conversion. As demonstrated in **Table S3**, a conversion ratio of >99 % was achieved at CPOA feeding rate of 1.1 mL·min^{-1} and 1 kU *Bm*GDH loading. Half of *Bm*GDH loading (0.5 kU) resulted in substrate accumulation and a final conversion ratio of merely 52.6 %. To achieve complete conversion of 250 mM CPOA, optimal *Qt*PDH:*Bm*GDH ratio was found to be either 1:1 or 1:2. It should be noted that the reaction time for ratio of 1:1 was approximately twice as long as that for 1:2. Therefore, subsequent reactions were performed at a ratio of 1:2.

Based on above optimized substrate feeding rate and enzyme loadings, reactions at enhanced CPOA concentration of 0.25−1.5 mol·L^{-1} were performed. As shown in Table 2, a complete and efficient amination reaction could be achieved at 0.25−1.0 mol·L^{-1} CPOA within 2–5 h. However, at 1.5 mol·L^{-1}, merely 73.5 % conversion was obtained at 12 h. At substrate concentration of 1.0 mol·L^{-1}, *Qt*PDH and *Bm*GDH loadings of 1 kU and 2 kU, a remarkable productivity of 30.46 g·L^{-1}·h^{-1} was achieved with a S/C of 36.94 g·g^{-1}. Furthermore, a scaled-up reaction system of 0.65 L was carried out, and a complete conversion of 1.0 mol·L^{-1} CPOA (99 g) in 11.5 h was observed. After dilution and acidification, the reaction solution was purified using JK006 cationic resin, as shown in **Figure S13**. The collection solution was subjected to rotary evaporation and lyophilization to obtain 92 g product as white powder with a purity of 98 %. Finally, the product 2-Cl-Phe was recovered with an overall yield of 91 %.

4. Conclusion

In this study, a novel AADH from *Quasibacillus thermotolerans* was explored by gene mining. *Qt*PDH shares 83.7 % identity with its probe protein sequence *Bb*PDH, whereas has excellent thermostability with a half-life of 23 days at pH 8.5. *Qt*PDH could catalyze bulky aromatic substrates, such as indole-3-pyruvic acid and 3-(naphthalen-1-yl)-2-oxopropanoic acid, in addition to natural amino acid substrates. *Qt*PDH also exhibited activity towards α-keto esters and (*S*)-amine alcohols. *Qt*PDH catalyzed a complete asymmetric amination of CPOA to 2-Cl-Phe with an S/C of 36.94 g·g^{-1} and a STY of 30.46 g·L^{-1}·h^{-1}. This study provides an efficient approach for synthesizing 2-Cl-Phe using newly identified *Qt*PDH with excellent catalytic properties.

Availability of data and materials

The data involved in this study are all included in the article and the supplementary material.

Funding

This work was supported by the National Key R&D Program (2018YFA0901700), and the National Natural Science Foundation of China (22078127).

Compliance with ethical standards

Ethical statement

The study in this paper does not involve any study of the human rights and ethnic situation.

CRediT authorship contribution statement

Yudong Hu: Data curation, Formal analysis, Investigation, Methodology, Writing – original draft, Writing – review & editing. **Guochao Xu:** Funding acquisition, Supervision, Resources, Writing – review & editing. **Ye Ni:** Funding acquisition, Supervision, Resources, Writing – review & editing.

Declaration of Competing Interest

The authors declare that they have no known competing financial interests or personal relationships that could have appeared to influence the work reported in this paper.

Data Availability

Data will be made available on request.

Supplementary materials

Supplementary material associated with this article can be found, in the online version, at doi:10.1016/j.mcat.2023.113713.

References

[1] R.N. Patel, Biocatalytic synthesis of chiral alcohols and amino acids for development of pharmaceuticals, Biomolecules 3 (4) (2013) 741–777, https://doi.org/10.3390/biom3040741.

[2] M.T. Reetz, Biocatalysis in organic chemistry and biotechnology: past, present, and future, J. Am. Chem. Soc. 135 (34) (2013) 12480–12496, https://doi.org/10.1021/ja405051f.

[3] B. deLange, D.J. Hyett, P.J.D. Maas, D. Mink, F.B.J. vanAssema, N. Sereinig, A.H. M. deVries, J.G. deVries, Asymmetric synthesis of (S)-2-indolinecarboxylic acid by combining biocatalysis and homogeneous catalysis, ChemCatChem 3 (2) (2011) 289–292, https://doi.org/10.1002/cctc.201000435.

[4] D. Ma, Y. Zhang, J. Yao, S. Wu, F. Tao, Accelerating effect induced by the structure of α-amino acid in the copper-catalyzed coupling reaction of aryl halides with α-amino acids. Synthesis of benzolactam-V8, J. Am. Chem. Soc. 120 (48) (1998) 12459–12467, https://doi.org/10.1021/ja981662f.

[5] H. Zhang, Q. Cai, D. Ma, Amino acid promoted CuI-catalyzed C−N bond formation between aryl halides and amines or N-containing heterocycles, J. Org. Chem. 70 (13) (2005) 5164–5173, https://doi.org/10.1021/jo0504464.

[6] I.E. Kopka, D.N. Young, L.S. Lin, R.A. Mumford, P.A. Magriotis, M. MacCoss, S. G. Mills, G. Van Riper, E. McCauley, L.E. Egger, U. Kidambi, J.A. Schmidt, K. Lyons, R. Stearns, S. Vincent, A. Colletti, Z. Wang, S. Tong, J.Y. Wang, S. Zheng, K. Owens, D. Levorse, W.K. Hagmann, Substituted N-(3,5-dichlorobenzenesulfonyl)-L-prolyl-phenylalanine analogues as potent VLA-4 antagonists, Bioorg. Med. Chem. Lett. 12 (4) (2002) 637–640, https://doi.org/10.1016/s0960-894x(01)00821-6.

[7] J.F. Hyslop, S.L. Lovelock, P.W. Sutton, K.K. Brown, A.J.B. Watson, G.D. Roiban, Biocatalytic synthesis of chiral N-functionalized amino acids, Angew. Chem. Int. Ed. Engl. 57 (42) (2018) 13821–13824, https://doi.org/10.1002/anie.201806893.

[8] U.T. Bornscheuer, G.W. Huisman, R.J. Kazlauskas, S. Lutz, J.C. Moore, K. Robins, Engineering the third wave of biocatalysis, Nature 485 (7397) (2012) 185–194, https://doi.org/10.1038/nature11117.

[9] C.K. Savile, J.M. Janey, E.C. Mundorff, J.C. Moore, S. Tam, W.R. Jarvis, J. C. Colbeck, A. Krebber, F.J. Fleitz, J. Brands, P.N. Devine, G.W. Huisman, G. J. Hughes, Biocatalytic asymmetric synthesis of chiral amines from ketones applied to sitagliptin manufacture, Science 329 (5989) (2010) 305–309, https://doi.org/10.1126/science.1188934.

[10] R.Z. Han, X.D. Cao, H.H. Fang, J.E.Y. Zhou, Y. Ni, Structure-based engineering of omega-transaminase for enhanced catalytic efficiency toward (R)-(+)-1-(1-naphthyl)ethylamine synthesis, Mol. Catal. 502 (2021) 8, https://doi.org/10.1016/j.mcat.2020.111368.

[11] J.L. Galman, D. Gahloth, F. Parmeggiani, I. Slabu, D. Leys, N.J. Turner, Characterization of a putrescine transaminase from pseudomonas putida and its application to the synthesis of benzylamine derivatives, Front. Bioeng. Biotechnol. 6 (2018) 11, https://doi.org/10.3389/fbioe.2018.00205.

[12] N.J. Weise, S.T. Ahmed, F. Parmeggiani, E. Siirola, A. Pushpanath, U. Schell, N. J. Turner, Intensified biocatalytic production of enantiomerically pure halophenylalanines from acrylic acids using ammonium carbamate as the ammonia source, Catal. Sci. Technol. 6 (12) (2016) 4086–4089, https://doi.org/10.1039/c6cy00855k.

[13] S.L. Lovelock, N.J. Turner, Bacterial Anabaena variabilis phenylalanine ammonia lyase: a biocatalyst with broad substrate specificity, Bioorg. Med. Chem. 22 (20) (2014) 5555–5557, https://doi.org/10.1016/j.bmc.2014.06.035.

[14] Y. Cui, Y. Wang, W. Tian, Y. Bu, T. Li, X. Cui, T. Zhu, R. Li, B. Wu, Development of a versatile and efficient C–N lyase platform for asymmetric hydroamination via computational enzyme redesign, Nat. Catal. 4 (5) (2021) 364–373, https://doi.org/10.1038/s41929-021-00604-2.

[15] S.L. Lovelock, R.C. Lloyd, N.J. Turner, Phenylalanine ammonia lyase catalyzed synthesis of amino acids by an MIO- cofactor independent pathway, Angew. Chem. Int. Ed. Engl. 53 (18) (2014) 4652–4656, https://doi.org/10.1002/ange.201311061.

[16] A.L. Ahmad, P.C. Oh, S.R.A. Shukor, Synthesis of L-homophenylalanine via integrated membrane bioreactor: influence of pH on yield, Biochem. Eng. J. 52 (2-3) (2010) 296–300, https://doi.org/10.1016/j.bej.2010.08.010.

[17] T. Wu, X. Mu, Y. Xue, Y. Xu, Y. Nie, Structure-guided steric hindrance engineering of Bacillus badius phenylalanine dehydrogenase for efficient L-homophenylalanine synthesis, Biotechnol. Biofuels 14 (1) (2021) 207, https://doi.org/10.1186/s13068-021-02055-0.

[18] F. Paradisi, S. Collins, A.R. Maguire, P.C. Engel, Phenylalanine dehydrogenase mutants: efficient biocatalysts for synthesis of non-natural phenylalanine derivatives, J. Biotechnol. 128 (2) (2007) 408–411, https://doi.org/10.1016/j.jbiotec.2006.08.008.

[19] Y. Asano, Enzymatic synthesis of (S)-phenylalanine and related (S)-amino acids by phenylalanine dehydrogenase, Microbial. Enzymes Biotransform. (2005) 141–150, https://doi.org/10.1385/1-59259-846-3:141.

[20] P. Busca, F. Paradisi, E. Moynihan, A.R. Maguire, P.C. Engel, Enantioselective synthesis of non-natural amino acids using phenylalanine dehydrogenases modified by site-directed mutagenesis, Org. Biomol. Chem. 2 (18) (2004) 2684–2691, https://doi.org/10.1039/b406364c.

[21] Y. Asano, A. Nakazawa, K. Endo, Y. Hibino, M. Ohmori, N. Numao, K. Kondo, Phenylalanine dehydrogenase of Bacillus badius. Purification, characterization and gene cloning, Eur. J. Biochem. 168 (1987) 153–159, https://doi.org/10.1111/j.1432-1033.1987.tb13399.x.

[22] J. Cheng, G.C. Xu, R.Z. Han, J.J. Dong, Y. Ni, Efficient access to L-phenylglycine using a newly identified amino acid dehydrogenase from Bacillus clausii, RSC Adv. 6 (84) (2016) 80557–80563, https://doi.org/10.1039/c6ra17683f.

[23] E. Gasteiger, A. Gattiker, C. Hoogland, I. Ivanyi, R.D. Appel, A. Bairoch, ExPASy: the proteomics server for in-depth protein knowledge and analysis, Nucleic Acids Res. 31 (13) (2003) 3784–3788, https://doi.org/10.1093/nar/gkg563.

[24] M.P. Thompson, I. Penafiel, S.C. Cosgrove, N.J. Turner, Biocatalysis using immobilized enzymes in continuous flow for the synthesis of fine chemicals, Org. Process Res. Dev. 23 (1) (2019) 9–18, https://doi.org/10.1021/acs.oprd.8b00305.

[25] J.H. Tao, K. McGee, Development of a continuous enzymatic process for the preparation of (R)-3-(4-fluorophenyl)-2-hydroxy propionic acid, Org. Process Res. Dev. 6 (4) (2002) 520–524, https://doi.org/10.1021/op010232y.

[26] S. Tachibana, Y. Kuwamori, Y. Asano, Discrimination of aliphatic substrates by a single amino acid substitution in Bacillus badius and Bacillus sphaericus phenylalanine dehydrogenases, Biosci. Biotechnol. Biochem. 73 (3) (2009) 729–732, https://doi.org/10.1271/bbb.80626.

[27] L.J. Ye, H.H. Toh, Y. Yang, J.P. Adams, R. Snajdrova, Z. Li, Engineering of amine dehydrogenase for asymmetric reductive amination of ketone by evolving Rhodococcus phenylalanine dehydrogenase, ACS Catal. 5 (2) (2015) 1119–1122, https://doi.org/10.1039/d2cy00391k.

[28] J. Li, J. Pan, J. Zhang, J.-H. Xu, Stereoselective synthesis of L-tert-leucine by a newly cloned leucine dehydrogenase from Exiguobacterium sibiricum, J. Mol. Catal. B Enzym. 105 (2014) 11–17, https://doi.org/10.1016/j.molcatb.2014.03.010.

[29] M. Sharma, J. Mangas-Sanchez, N.J. Turner, G. Grogan, NAD(P)H-dependent dehydrogenases for the asymmetric reductive amination of ketones: structure, mechanism, evolution and application, Adv. Synth. Catal. 359 (12) (2017) 2011–2025, https://doi.org/10.1002/adsc.201700356.

[30] T. Oliveira, S. Panjikar, J.B. Carrigan, M. Hamza, M.A. Sharkey, P.C. Engel, A. R. Khan, Crystal structure of NAD+-dependent Peptoniphilus asaccharolyticus glutamate dehydrogenase reveals determinants of cofactor specificity, J. Struct. Biol. 177 (2) (2012) 543–552, https://doi.org/10.1016/j.jsb.2011.10.006.

[31] J.B.T. Norbert, M.W. Brunhuber, John S. Blanchard, J.L. Vanhooke, Rhodococcus L-phenylalanine dehydrogenase: kinetics, mechanism, and structural basis for catalytic specifity, Biochemistry 39 (31) (2000) 9174–9187, https://doi.org/10.1021/bi000494c.

[32] F. Parmeggiani, S.T. Ahmed, M.P. Thompson, N.J. Weise, J.L. Galman, D. Gahloth, M.S. Dunstan, D. Leys, N.J. Turner, Single-biocatalyst synthesis of enantiopure D-arylalanines exploiting an engineered D-amino acid dehydrogenase, Adv. Synth. Catal. 358 (20) (2016) 3298–3306, https://doi.org/10.1002/adsc.201600682.

[33] J. Zhang, S. Tao, B. Zhang, X. Wu, Y. Chen, Microparticle-based strategy for controlled release of substrate for the biocatalytic preparation of L-homophenylalanine, ACS Catal. 4 (5) (2014) 1584–1587, https://doi.org/10.1021/cs4011919.